SCIENTIFIC REPORTS

OPEN

The electron distribution in the "activated" state of cytochrome *c* oxidase

Received: 20 November 2017
Accepted: 26 April 2018
Published online: 14 May 2018

Jóhanna Vilhjálmsdóttir[1], Robert B. Gennis[2] & Peter Brzezinski[1]

Cytochrome *c* oxidase catalyzes reduction of O_2 to H_2O at a catalytic site that is composed of a copper ion and heme group. The reaction is linked to translocation of four protons across the membrane for each O_2 reduced to water. The free energy associated with electron transfer to the catalytic site is unequal for the four electron-transfer events. Most notably, the free energy associated with reduction of the catalytic site in the oxidized cytochrome *c* oxidase (state O) is not sufficient for proton pumping across the energized membrane. Yet, this electron transfer is mechanistically linked to proton pumping. To resolve this apparent discrepancy, a high-energy oxidized state (denoted O_H) was postulated and suggested to be populated only during catalytic turnover. The difference between states O and O_H was suggested to be manifested in an elevated midpoint potential of Cu_B in the latter. This proposal predicts that one-electron reduction of cytochrome *c* oxidase after its oxidation would yield re-reduction of essentially only Cu_B. Here, we investigated this process and found ~5% and ~6% reduction of heme a_3 and Cu_B, respectively, i.e. the apparent redox potentials for heme a_3 and Cu_B are lower than that of heme *a*.

The electrochemical proton gradient across the inner mitochondrial or bacterial cytoplasmic membrane in aerobic organisms is maintained by a series of membrane-bound redox-driven proton pumps. The final electron acceptor, O_2, binds to cytochrome *c* oxidase (Cyt*c*O) at a bimetallic heme a_3-Cu_B catalytic site where it is reduced by four electrons to water (Fig. 1a). During turnover of Cyt*c*O, electrons are transferred one-by-one from a water-soluble or membrane-associated cyt. *c* consecutively to the primary electron acceptor, Cu_A, the secondary acceptor heme *a* and the catalytic site. The Cyt*c*O links this electron transfer to proton pumping from the more negative (*N*) to the more positive (*P*) side of the membrane with an average stoichiometry of one pumped proton per electron transferred to the catalytic site. Thus, the overall reaction is:

$$4e^-_P + 8H^+_N + O_2 \rightarrow 2H_2O + 4H^+_P \quad (1)$$

where the subscripts *P* and *N* refer to the two sides of the membrane. The free energy for reduction of O_2 by cyt. *c* is ~2 eV, which is used to move 8 charges across the membrane; 4 protons that are pumped across the membrane and, 4 electrons and 4 protons that are transferred from opposite sides of the membrane resulting in a charge separation (summarized in[1]).

A number of distinct intermediate states have been identified and characterized during Cyt*c*O turnover (Fig. 1b). Consecutive transfer of two electrons to the oxidized Cyt*c*O (denoted **O**) yields formation of the one- (denoted **E**) and two- (denoted **R**) electron reduced catalytic site. When heme a_3 and Cu_B are reduced, O_2 binds to the heme iron after which the O-O bond is broken to form a ferryl state called "peroxy" for historical reasons (denoted $\mathbf{P_M}$). Transfer of an additional electron and a proton to $\mathbf{P_M}$, results in formation of the ferryl state, **F**. Further transfer of an electron and a proton to **F** yields the oxidized Cyt*c*O ($\mathbf{O_H}$, see below). The overall process has been reviewed in the past[1–14] and it is summarized in Fig. 1b.

Early studies indicated that the free energy from O_2 reduction is not released evenly in the four electron-transfer reactions, but the majority of this free energy was found to be liberated in the $\mathbf{P_M} \rightarrow \mathbf{F}$ and $\mathbf{F} \rightarrow \mathbf{O}$ reaction steps[15]. Furthermore, elegant studies performed by Wikström suggested that proton pumping is coupled

[1]Department of Biochemistry and Biophysics, The Arrhenius Laboratories for Natural Sciences, Stockholm University, SE-106 91, Stockholm, Sweden. [2]Department of Biochemistry, University of Illinois at Urbana Champaign, Urbana, Illinois, 61801, United States. Correspondence and requests for materials should be addressed to P.B. (email: peterb@dbb.su.se)

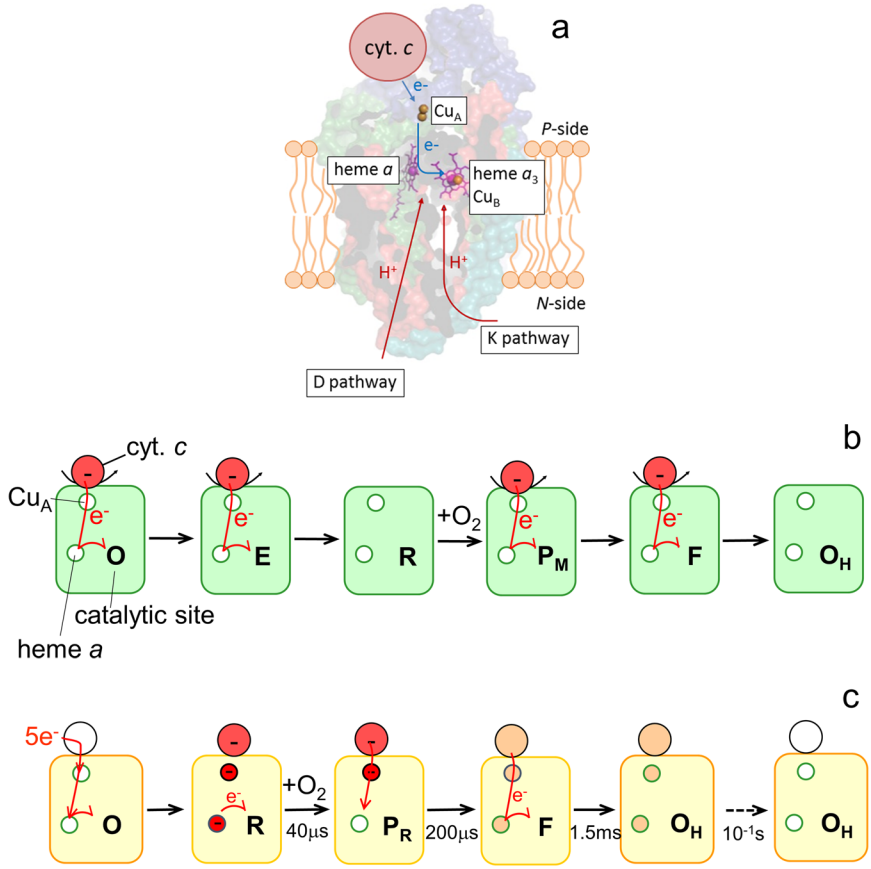

Figure 1. Experimental system and the studied reaction. (**a**) Cyt*c*O accommodates four redox-active centers: Cu_A, heme *a* and the catalytic site composed of heme a_3 and Cu_B, that upon reduction each bind one electron. The cyt. *c*-Cyt*c*O electrostatic complex accommodates in total five electrons in the reduced state. Two proton-uptake pathways, called D and K are indicated in the figure, but not discussed in the text. (**b**) Turnover of Cyt*c*O. One electron at a time is donated from cyt. *c* to Cyt*c*O. The initial state is the "relaxed" oxidized state. Consecutive addition of two electrons yields the two-electron reduced catalytic site which binds O_2 to form the peroxy state P_M. Reduction of P_M yields F, which is then reduced to form the "activated" oxidized state, O_H. This state is then reduced by cyt. *c*. (**c**) Reaction studied in this work. The oxidized cyt. *c*-Cyt*c*O complex is reduced by 5 electrons. Upon initiation of the reaction (with a laser flash, not shown), O_2 binds to the catalytic site and an electron is transferred from heme *a* to the catalytic site to form the peroxy state, P_R. This step is followed in time by formation of the ferryl state, F, which occurs over the same time scale as electron equilibration among Cu_A/cyt. *c* and heme *a*. Electron transfer from this equilibrium to the catalytic site leads to formation of state O_H. Over a longer time scale of ~0.1 s an electron equilibrates between the Cyt*c*O molecules via the bound cyt. *c* to eventually yield oxidized Cyt*c*O. Note that proton-transfer reactions are not indicated in the Figure.

only to these two steps[16], which stimulated Wikström and colleagues to propose a detailed molecular model based on these findings[17]. According to this model, two protons would be pumped in each of the reactions $\mathbf{P_M} \rightarrow \mathbf{F}$ and $\mathbf{F} \rightarrow \mathbf{O}$, while no proton pumping would be observed upon reduction of the Cyt*c*O, i.e. $\mathbf{O} \rightarrow \mathbf{E} \rightarrow \mathbf{P_M}$. Later, a novel kinetic approach was used to obtain data[18] that resulted in re-evaluation of the model to yield a scenario where one proton is pumped in each of the four reaction steps that involve electron transfer to the catalytic site[19].

A key aspect of the new model was postulation of a "high-energy" metastable oxidized form of the Cyt*c*O that would presumably differ in structure from the oxidized "as isolated" (**O**) state. The state is denoted $\mathbf{O_H}$ and it is assumed to be formed as a product of the $\mathbf{F} \rightarrow \mathbf{O_H}$ reaction (below we denote by $\mathbf{O_H}$ the oxidized state that is formed after re-oxidation of the reduced Cyt*c*O independently of the properties of this state)[18]. According to this scenario part of the free energy released in $\mathbf{P_M} \rightarrow \mathbf{F}$ and $\mathbf{F} \rightarrow \mathbf{O_H}$ would be conserved in the $\mathbf{O_H}$ state to be used during subsequent reduction of the Cyt*c*O, i.e. the reaction sequence $\mathbf{O_H} \rightarrow \mathbf{E} \rightarrow \mathbf{P_M}$ would be more exergonic than $\mathbf{O} \rightarrow \mathbf{E} \rightarrow \mathbf{P_M}$. The question arises: what is the difference between states **O** and $\mathbf{O_H}$?

Postulation of state $\mathbf{O_H}$ also found support in an experimental observation: when starting from the fully oxidized Cyt*c*O (**O**) the free energy associated with electron transfer from cyt. *c* to heme a_3-Cu_B, before O_2 binds, is too small to drive proton translocation (see Kaila *et al.*[1]). Consequently, one possible difference between the "as isolated" state **O** and state $\mathbf{O_H}$ could be that in the latter the midpoint potentials of heme a_3 and Cu_B are higher than those in state **O**[19,20]. Indeed, data from experimental[21] and theoretical[22] studies suggested that the mid-point potential of Cu_B is significantly elevated in state $\mathbf{O_H}$. Furthermore, Blomberg and Siegbahn found that the

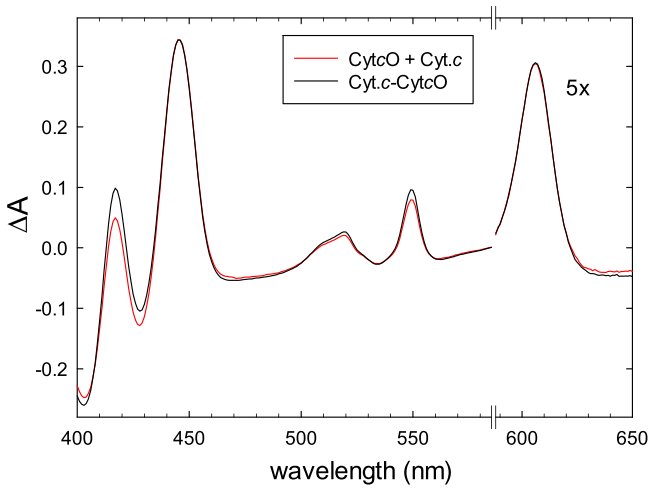

Figure 2. Absorbance difference spectra. A comparison of reduced minus oxidized difference spectra of the Cyt*c*O-cyt. *c* complex (black) and the sum of the reduced minus oxidized difference spectra of Cyt*c*O and cyt. *c* (red), respectively. Spectra of the oxidized states were recorded first and then the atmosphere in the cuvette was replaced for N_2 after which the samples were reduced with ascorbate (2 mM) and hexaammineruthenium(II) chloride (1 μM). Reduction of the samples was followed in time by recording spectra over ~2 hours until no further changes were observed. The data to the right of the axis break have been multiplied by a factor of five. The concentrations of Cyt*c*O and cyt. *c* were ~3 μM and ~5 μM, respectively, in 50 mM HEPES (pH 7.5), 0.05% DDM and 100 μM EDTA.

inherent midpoint potential of Cu_B is high during catalytic turnover, and that in the resting oxidized state a slow protonation process may cause a significant decrease of the proton-coupled reduction potential[23]. As discussed in the paper by Belevich *et al.*[21], there are conflicting experimental data regarding possible differences in the Cu_B midpoint potentials between states **O** and $\mathbf{O_H}$. For example, Jancura *et al.*[24] did not observe any spectral or kinetic differences between the $\mathbf{O_H}$ and **O** forms of Cyt*c*O. Brand *et al.*[25] prepared Cyt*c*O in the **O** and $\mathbf{O_H}$ states, respectively, and then added one electron to each of the samples. They found that the extent of electron transfer from heme *a* to the catalytic site was relatively small and the same in both states, which indicated that the midpoint potential of Cu_B was not raised in state $\mathbf{O_H}$.

In the present study, we investigated the reaction of the reduced *Rhodobacter sphaeroides* Cyt*c*O with O_2 in the absence and presence, respectively, of cyt. *c* at low ionic strength. In the latter case a cyt. *c*-Cyt*c*O electrostatic complex is formed (see Fig. 1a,c). This arrangement contrasts the earlier studies in that it resembles the *in vivo* situation where electrons are continuously fed into Cyt*c*O from the donor cyt. *c*. The cyt. *c*-Cyt*c*O complex accommodates five electrons. Upon binding of O_2 four electrons are transferred to form H_2O yielding the oxidized Cyt*c*O, presumably in state $\mathbf{O_H}$. Then the "fifth electron" can equilibrate among the five sites cyt. *c*, Cu_A, heme *a*, heme a_3 and Cu_B[26–28]. We reasoned that if in state $\mathbf{O_H}$ the Cu_B midpoint potential would be elevated, this fifth electron would be transferred to Cu_B. The data show that this was not the case and in ~90% of Cyt*c*Os the fifth electron was distributed among sites cyt. *c*, Cu_A and heme *a* with the largest fraction at heme *a*.

Results and Discussion

Spectral analysis. To determine whether or not binding of cyt. *c* to Cyt*c*O affects the spectral properties of the hemes, we recorded the reduced - oxidized difference spectra of each of the isolated proteins (cyt. *c* and Cyt*c*O) as well as of a mixture of the two at low ionic strength (i.e. the cyt. *c*-Cyt*c*O complex). As seen in Fig. 2, the sum of the cyt. *c* and Cyt*c*O difference spectra was essentially equal to that of the mixture, except for a small increase in the 550 nm absorbance peak upon forming the cyt. *c*-Cyt*c*O complex.

Reaction of Cyt*c*O with O_2. The reduced Cyt*c*O carries four electron equivalents. Thus, upon reaction with O_2 the Cyt*c*O becomes fully oxidized while O_2 is reduced to H_2O. The anaerobic samples were mixed with an O_2-saturated solution in a stopped-flow apparatus. After ~200 ms the CO ligand was dissociated by means of a short laser flash, which initiates the reaction of the reduced Cyt*c*O with O_2. In the absence of cyt. *c* (black traces in Fig. 3) the reaction exhibits a number of distinct kinetic steps, while populating states in which O_2 is progressively reduced and protonated to eventually form H_2O. The details of the reaction sequence have been described in the past[1,4,5,29,30] and it is outlined in Fig. 1c.

At 445 nm and 605 nm the main contribution to the absorbance changes is from both hemes *a* and a_3. At 830 nm and 550 nm the main contribution is from Cu_A and cyt. *c*, respectively. The $\mathbf{A} \rightarrow \mathbf{P_R}$ and $\mathbf{F} \rightarrow \mathbf{O}$ reactions are seen as a decrease in absorbance with time constants of ~40 μs and ~1.5 ms (Fig. 3a,b), respectively, at both 445 nm and 605 nm. The $\mathbf{P_R} \rightarrow \mathbf{F}$ reaction is not seen at these wavelengths, but fractional oxidation of Cu_A that is linked in time to the $\mathbf{P_R} \rightarrow \mathbf{F}$ reaction[31] is seen at 830 nm where we observed an increase in absorbance with a time constant of ~200 μs (Fig. 3c). Also the remaining oxidation of Cu_A, linked in time to the $\mathbf{F} \rightarrow \mathbf{O_H}$ reaction, is seen as a further increase in absorbance at 830 nm. We did not observe any absorbance changes at 550 nm in the

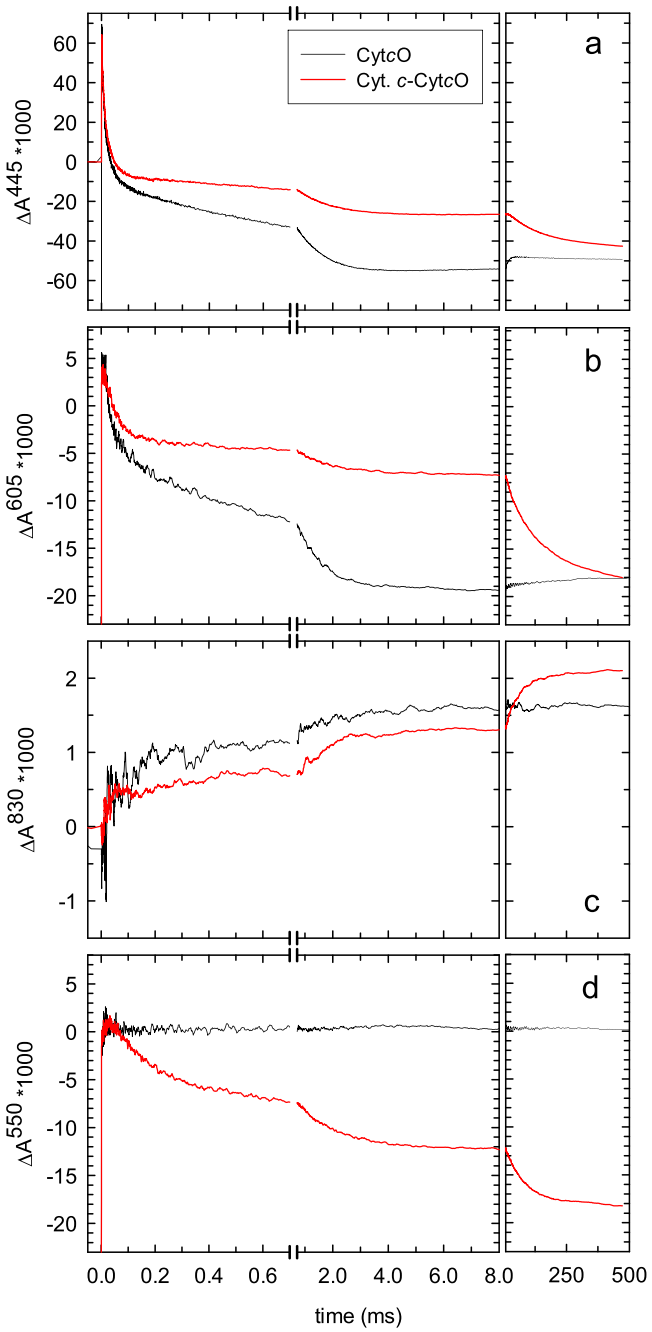

Figure 3. Kinetics of absorbance changes upon reaction with O_2. The four-electron reduced Cyt*c*O (black traces) or the five-electron-reduced cyt. *c*-Cyt*c*O complex (red traces) was mixed with an O_2-saturated buffer solution. About 200 ms after mixing with the O_2-containing buffer, at time = 0, the CO-ligand was removed by a laser flash. The four-electron complex becomes oxidized over a time scale of 8 ms (left-hand side boxes). At 445 nm (**a**) the main contribution is from redox changes at hemes *a* and a_3. At 605 nm (**b**) the main contribution is from redox changes at heme *a* (80%) and the remaining fraction originates from changes at heme a_3. At 830 nm (**c**) the main contribution is from Cu_A where an increase in absorbance is associated with oxidation. At 550 nm (**d**) the main contribution is from redox changes at cyt. *c*. At 445 nm and 605 nm, the rapid change in absorbance at $t = 0$ is associated with CO dissociation. It is followed in time by a decrease in absorbance associated with binding of O_2 ($\tau \cong 10\,\mu s$), formation of the $\mathbf{P_R}$ state ($\tau \cong 40\,\mu s$) and oxidation of the Cyt*c*O ($\tau \cong 1.5$ ms). The $\mathbf{P_R} \rightarrow \mathbf{F}$ reaction is not seen at these wavelengths. At 830 nm two components are seen with time constants of 200 µs ($\mathbf{P_R} \rightarrow \mathbf{F}$) and 1.5 ms ($\mathbf{F} \rightarrow \mathbf{O}$). Oxidation of cyt. *c* occurs over the same time scale. In the presence of cyt. *c* absorbance changes attributed to the Cyt*c*O (panels a–c) were smaller because the redox sites were re-reduced by cyt. *c* during the course of the reaction. Over a time scale of ~500 ms (right-hand side boxes) all redox sites become oxidized. The small increase in absorbance over this time scale in the absence of cyt. *c* is due to small fractional re-reduction of Cyt*c*O by ascorbate. Experimental conditions after mixing: 1.1 µM Cyt*c*O, 20 mM HEPES at pH 7.5, 0.05% DDM, 100 µM EDTA, 2 mM ascorbate, 1 µM hexa-ammine-ruthenium(II) chloride, 1 mM O_2 at ~22 °C (black trace). The red traces are averages of three traces obtained

under the following conditions: [cyt. *c*]/[Cyt*c*O] in μM (*i*) 2.1/1.6, (*ii*) 1.5/1.3, (*iii*) 1.7/1.3. The mixing ratio was 1:5 with an oxygen-saturated buffer solution (20 mM HEPES at pH 7.5). All traces have been scaled to 1 μM reacting Cyt*c*O based on the rapid change in absorbance at 445 nm at $t = 0$. A laser artifact at $t = 0$ has been truncated for clarity.

absence of cyt. *c*, which shows that at this wavelength the contribution from redox changes of Cyt*c*O is negligible (Fig. 3d, black trace).

Over a longer time scale we observed a slight re-reduction of hemes *a* and a_3, seen as a small increase in absorbance at 445 nm and 605 nm (see right-hand side boxes of panels a and b).

Reaction of the cyt. *c*-Cyt*c*O complex with O_2. A mixture of cyt. *c* and Cyt*c*O, in a low-ionic strength solution (see Materials and Methods), was reduced and incubated under an atmosphere of CO. The cyt. *c* was added at a slight excess to Cyt*c*O (1.2–1.3 cyt. *c*/Cyt*c*O) to assure formation of the cyt. *c*-Cyt*c*O complex in the major fraction of the population (see below). We first discuss the absorbance changes over a time scale of 8 ms (black traces in Fig. 3). Over this time scale four electrons are delivered from Cyt*c*O to O_2, as discussed above.

When cyt. *c* is bound to Cyt*c*O an electron is transferred from cyt. *c* to Cu_A upon the first, fractional oxidation of Cu_A, i.e. during the $\mathbf{P_R} \rightarrow \mathbf{F}$ reaction ($\tau \cong 200\,\mu s$), and then during the $\mathbf{F} \rightarrow \mathbf{O_H}$ reaction ($\tau \cong 1.5$ ms) while Cu_A/heme *a* are oxidized further (red traces in Fig. 3)[26–28]. These oxidation reactions are seen as a decrease in absorbance at 550 nm with time constants of ~200 μs and ~1.5 ms, respectively. All other absorbance changes over a time scale of 8 ms were diminished in the presence of cyt. *c*, reflecting re-reduction of the Cyt*c*O redox sites by cyt. *c* (compare the red and black traces in Fig. 3a–c).

The absorption coefficients of the redox sites at the measured wavelengths are listed in Table 1. All data in Fig. 3 were scaled to 1 μM reacting Cyt*c*O, based on the absorption coefficient for the CO-dissociation absorbance change at 445 nm. This normalization was only done to simplify comparison of the data at different wavelengths and it does not influence the analysis below.

Further oxidation of the cyt. *c*-Cyt*c*O complex after reaction with O_2. In the five-electron cyt. *c*-Cyt*c*O system the single remaining electron after oxidation of the Cyt*c*O is not rapidly transferred to the excess oxygen (i.e. to a second O_2) because O_2 does not bind to the catalytic site when it is reduced by only one electron. Instead, oxidation of the hemes occurred over a longer time scale of ~500 ms, see right-hand side boxes in Fig. 3. This process may involve either (*i*) transfer of the electron to the optically silent Cu_B, or (*ii*) electron exchange between the Cyt*c*O molecules, via cyt. *c*, eventually yielding a thermodynamically stable state. The oxidation state of the Cyt*c*O catalytic site in this stable state would depend on the number of electrons transferred to the specific enzyme molecule. The most likely scenario is that an electron is exchanged between two Cyt*c*Os such that one molecule becomes oxidized and the other forms state $\mathbf{P_M}$.

To discriminate between these two scenarios we reasoned that in case (*i*) the time constant of the slowest oxidation reaction would be independent of the Cyt*c*O concentration while in case (*ii*) this time constant would decrease upon dilution because the reaction involves electron exchange between Cyt*c*O molecules mediated via cyt. *c*. As seen in Fig. 4, the time constant of the slowest component increased from ~75 ms to ~300 ms upon increasing the dilution of the Cyt*c*O-cyt. *c* sample with the O_2-containing buffer from 1:1 to 1:5. This observation indicates that the slowest component is due to electron exchange between Cyt*c*O molecules according to scenario (*ii*).

At 550 nm we observed a decrease in absorbance in the time range 8-500 ms (see Fig. 3d) that was added on top of the oxidation of the fraction reduced cyt. *c* in the cyt. *c*-Cyt*c*O complex. This signal was observed because there was an excess of 1.2–1.3 cyt. *c* compared to Cyt*c*O. Over this longer time scale this excess cyt. *c* in solution, became fully oxidized.

For the Cu_A absorbance changes at 830 nm (Fig. 3c) the absorbance reached a higher level with than without cyt. *c* at 500 ms, which is discussed below.

Analysis of the data. We define the absorbance difference, at wavelength λ, after *x* ms and immediately after the flash, i.e. at time $= 0^+$: $\Delta A^{\lambda}(x) = A^{\lambda}(t = x\text{ ms}) - A^{\lambda}(t = 0^+)$. As already indicated above, in the absence of cyt. *c*, $\Delta A^{\lambda}(8)$ reflects oxidation of the reduced Cyt*c*O. We note that a comparison of this absorbance change at e.g. 445 nm and 605 nm, and that associated with CO-dissociation typically deviates from the equivalent differences seen in static spectra (Table 1). Therefore, we found that the most reliable approach to analyze the absorbance changes associated with oxidation of hemes *a* and a_3 is to compare $\Delta A^{445}(8)$ and $\Delta A^{605}(8)$ with and without cyt. *c* added. This approach does not require the knowledge of absorption coefficients of hemes *a* and a_3, only their relative contribution must be known. As seen in Table 1, at 605 nm hemes *a* and a_3 contribute with 80% and 20%[32,33], respectively. At 445 nm we used the relative contributions determined by Vanneste[33]: 66% and 34% for hemes a_3 and *a*, respectively. The relative contributions determined by Liao *et al.*[32] differed from these values, but the use of these values yields the same conclusions (see below).

The fractions hemes *a* and a_3 ($\delta(a)$ and $\delta(a_3)$, respectively) that become oxidized after 8 ms in the presence of cyt. *c* are determined from:

$$\frac{\Delta A^{445}_{+\text{cyt.}c}(8)}{\Delta A^{445}(8)} = 0.34\delta(a) + 0.66\,\delta(a_3) = 0.75 \quad (2)$$

Redox site or reaction	Δε $mM^{-1}cm^{-1}$	wavelength (nm)	Reference
Cyt*c*O-CO-Cyt*c*O	67	445	[33]
cyt. *c*	21.1	550	[46]
Cu_A	2.3	830	[47]
	1.6		[34]
heme a_3	112	445	[33]
	82.3	444	[32]
heme *a*	57	445	[33]
	66.4	446	[32]
heme *a*	20.5	605	[33]
	18.6		[32]
heme a_3	4.8	605	[33]
	4.6		[32]

Table 1. Reduced minus oxidized difference absorption coefficients (Δε) of the redox sites, except the first line where the Δε is given for CO binding to the reduced heme a_3.

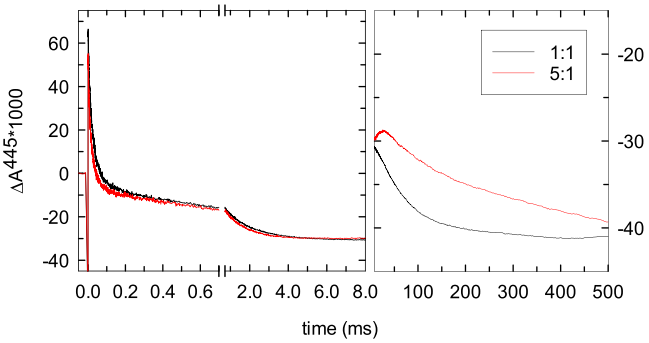

Figure 4. Kinetics of absorbance changes upon reaction with O_2 upon dilution. The experiment is the same as that shown in Fig. 3, but the Cyt*c*O-containing sample was mixed 1:1 (black) or 1:5 (red) with the O_2-containing buffer. Note the different absorbance scales in the left and right parts of the graph, respectively. The concentrations of Cyt*c*O and cyt. *c* were 5 µM and 7.5 µM, respectively.

$$\frac{\Delta A^{605}_{+\text{cyt.}c}(8)}{\Delta A^{605}(8)} = 0.80\delta(a) + 0.20\delta(a_3) = 0.50 \quad (3)$$

which yields $\delta(a) = 0.40 \pm 0.04$ and $\delta(a_3) = 0.94 \pm 0.06$ (SD, 3 measurements). In other words, ~60% of heme *a*, but only ~6% of heme a_3 become re-reduced when cyt. *c* is present. When using the relative contributions of hemes *a* and a_3, respectively, based on the absorption coefficients determined by Liao *et al.*[32] (see Table 1), the corresponding values would be $\delta(a) \cong 0.5$ and $\delta(a_3) \cong 1$, i.e. ~50% re-reduced heme *a* and no heme a_3 re-reduced.

Next, we calculate the fraction Cu_A that becomes re-reduced in the presence of cyt. *c* from the absorbance changes at 830 nm (Fig. 3c). At this wavelength oxidation of Cu_A leads to an increase in absorbance.

We compare the absorbance levels after 8 ms obtained in the absence and presence of cyt. *c*: $\frac{\Delta A^{830}_{+\text{cyt.}c}(8)}{\Delta A^{830}(8)} = 0.85 \pm 0.08$ (SD, three measurements), which yields ~15% re-reduced Cu_A when cyt. *c* is present.

We note that the absorbance levels at 830 nm after 500 ms in the presence and absence of cyt. *c* differ. This difference is most likely due to contribution of state $\mathbf{P_M}$, at 830 nm[34], formed at the catalytic site after electron exchange between the Cyt*c*Os in the presence of cyt. *c* (see explanation above).

The fraction oxidized cyt. *c* is calculated from the absorbance changes at 550 nm (Fig. 3d). We calculated the fraction from the ratio of absorbance changes at 500 ms (full oxidation of the cyt. *c* pool) and 8 ms, respectively, assuming that the fraction oxidized cyt. *c* over the time scale of 8 ms reflects cyt. *c* that was bound in complex with Cyt*c*O.

The fraction oxidized cyt. *c* after 8 ms, $\frac{\Delta A^{550}_{+\text{cyt.}c}(8)}{\Delta A^{550}_{+\text{cyt.}c}(500)}$ is 0.68. This number must be scaled for the molar excess cyt. *c* as compared to Cyt*c*O, which is 1.2 (in the experiment shown in Fig. 3d). Thus, assuming a 1:1 cyt. *c*-Cyt*c*O complex, the absorbance changes at 8 ms yield oxidation of 84 ± 7% (SD, 3 measurements) of the bound cyt. *c*. The occupancy of the cyt. *c*-binding site is not known, but because the degree of cyt. *c* oxidation is close to unity, the assumption of a 1:1 cyt. *c*:Cyt*c*O complex is at least approximately correct.

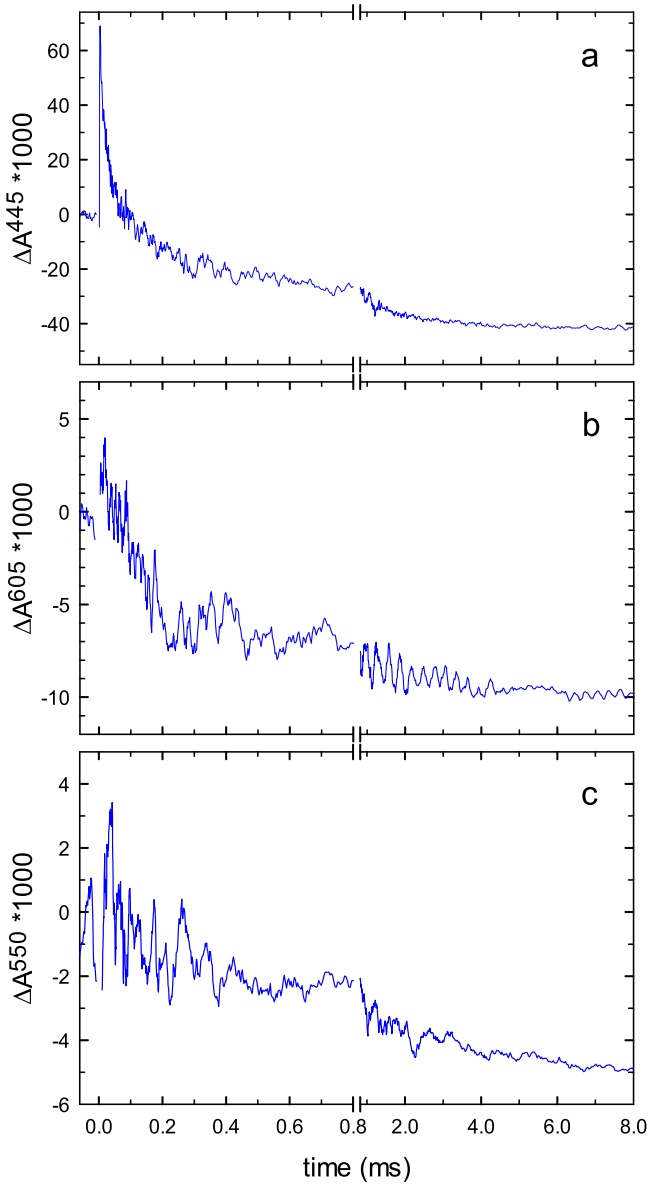

Figure 5. Reaction of membrane fragments with O_2. The experiment is the same as that shown in Fig. 3. Absorbance changes were monitored at 445 nm (**a**) 605 nm (**b**) and 550 nm (**c**) Experimental conditions after mixing: *R. sphaeroides* membranes (~2 μM Cyt*c*O, calculated from the reduced minus oxidized difference spectrum) in 20 mM HEPES (pH 7.5), 100 μM EDTA and 1 mM O_2 at ~22 °C. The mixing ratio was 1:1 with an oxygen-saturated buffer (20 mM HEPES pH 7.5). The traces have been scaled to 1 μM reacting Cyt*c*O. A laser artifact at $t = 0$ has been truncated for clarity.

To test whether or not the presence of detergent could alter the midpoint potentials of Cyt*c*O in state $\mathbf{O_H}$, we also repeated the experiments with native membranes from *R. sphaeroides* (Fig. 5). Due to light scattering of the membrane fragment the signal-to-noise ratio in these measurements was much smaller than that seen with detergent-solubilized Cyt*c*O. Therefore, we had to exclude data at 830 nm where the absorbance changes associated with redox changes at Cu_A are very small (see Table 1). We observed a smaller degree of cyt. *c* oxidation over ~8 ms, presumably because part of cyt. *c* binds to the membrane fragments, being inaccessible to Cyt*c*O. Nevertheless, we could estimate the degree of cyt. *c* oxidation and reduction of hemes *a* and a_3. The fraction oxidized cyt. *c* per Cyt*c*O was ~0.4 (Fig. 5c), based on a comparison with the data in Fig. 3d. The fraction reduced hemes *a* and a_3 was estimated using Eqs (1 and 2) above and the absorbance differences $\Delta A^{445}(8)$ and $\Delta A^{605}(8)$ in Fig. 5a,b. These data indicate that at 8 ms after initiation of the reaction, heme a_3 is not reduced while heme *a* is essentially fully reduced, which is qualitatively consistent with the data obtained with Cyt*c*O in detergent solution.

Interpretation of the data obtained with detergent-solubilized Cyt*c*O is summarized in the illustration in Fig. 6. We found that at the end of the initial oxidation of the Cyt*c*O, i.e. after 8 ms, the fraction reduced cyt. *c* is 0.16. In other words, we assume that 0.84 electrons reside among the four redox sites of Cyt*c*O. The reduction levels of hemes *a* and a_3 were 0.60 and 0.06, respectively, while that of Cu_A was 0.15. These numbers are obtained

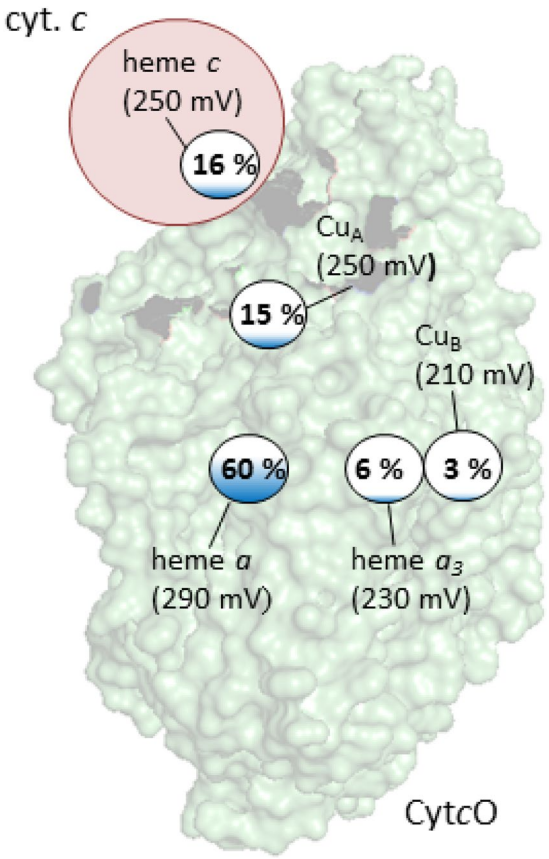

Figure 6. Summary of the data. The redox state of the co-factors is indicated with color. The fraction color in the small circles reflects the degree of reduction of each redox site. The apparent redox potentials were estimated from the fractions reduced redox sites assuming a midpoint potential of 250 mV for Cu_A. The numbers are based on the assumption that the cyt. *c*-Cyt*c*O complex accommodates five redox sites and that each site can accommodate one electron. No interactions between the redox sites are considered (see text).

from the measured absorbance changes. When adding these fractions reduced hemes *a* and a_3 and Cu_A we obtain 0.81. Because 0.84 electrons reside at Cyt*c*O (based on the degree of oxidation of cyt. *c*), the fraction reduced Cu_B is 0.03. It should be noted that this number is not measured directly because Cu_B is optically silent. It is calculated based on the assumption that the cyt. *c*-Cyt*c*O complex comprises five redox-active centers and that each of these sites can harbor one electron.

On the basis of this distribution of the fifth electron among the five redox sites cyt. *c*, Cu_A, heme *a*, heme a_3 and Cu_B, and assuming a midpoint potential of 250 mV for Cu_A[35], we estimate the apparent redox potentials of the redox sites in Cyt*c*O in state $\mathbf{O_H}$ (Fig. 6). We refer to "apparent" redox potentials because the analysis reflects only the distribution of a single electron after 500 ms in the five-electron system (among five sites). Because interactions between the redox sites are not considered (see[35,36]), the values differ from those obtained in redox titrations, which typically yield a higher midpoint potential for the catalytic site heme (here heme a_3) than for the intermediate electron acceptor (here heme *a*)[35,36], although in many bacterial oxidases the difference between the midpoint potentials is reversed[37]. Furthermore, because a single electron equilibrates among the five redox sites, the situation differs from a redox titration[38]. The purpose of the exercise to calculate the apparent redox potentials is not to provide the values, only to indicate that the apparent redox potential of Cu_B is not higher than that of any other site after reaction of the Cyt*c*O with O_2. The main conclusion is that the fifth electron is not found at the catalytic site.

Belevich and colleagues[21] concluded that upon injection of a single electron to state $\mathbf{O_H}$ less than 2% heme *a* was reduced and that the midpoint potential of Cu_B was raised to a value at least 100 mV higher than that of heme *a*. This contrasts the 60% reduced heme *a* observed here and we did not find an increased midpoint potential of Cu_B. One difference between our study and that of Belevich *et al.* is the different experimental approach; we used cyt. *c* as the electron donor while Belevich *et al.* used a Ru-complex excited by light. Even though the binding geometry and overall charge of these two electron donors differ, the differences are not likely to explain the discrepancy in the Cu_B midpoint potentials because of the significant distance between the site where the electron donor binds and Cu_B. Belevich and colleagues[21] discussed the discrepancy between their results and those obtained in other laboratories prior to the present study, and suggested that they may originate from exposure of the Cyt*c*O to detergent or removal of phospholipids during enzyme isolation. As discussed above, we did not find any additional reduction of the catalytic site with Cyt*c*O in its native lipid environment.

In earlier studies using an identical experimental approach to that used here[39,40] we did observe differences between Cyt*c*O that was reconstituted in liposomes and in detergent. However, these differences were mainly observed for the kinetics of reactions that are associated with proton uptake from solution, presumably due to interaction of lipids with groups near the entry point of the Cyt*c*O proton pathways[40].

The experimental approach used here reflects the conditions in the native system where cyt. *c* is the electron donor. Yet, one may argue that in our experiments the electron from cyt. *c* was transferred over a time scale that is shorter than that of $\mathbf{O_H}$ formation, i.e., an alternative explanation is that the state formed is not $\mathbf{O_H}$. State **O** is defined as the "relaxed form" of the oxidized Cyt*c*O, reached after long time without turnover, i.e. not the transient state visited in the experiments described here. Consequently, if we assume that $\mathbf{O_H}$ is not formed here, we would have to assume a third oxidized state. Furthermore, we would have to postulate that formation of $\mathbf{O_H}$ requires a delay between oxidation and re-reduction of the Cyt*c*O. However, the concentration of O_2 in mammalian tissues is only a few μM[41], which suggests that at steady state heme *a*/Cu_A would be at least partly reduced, resembling the states visited in the current study, as also indicated in[42]. We also note that in the experiments described by Belevich and colleagues[21] the delay between oxidation and injection of the fifth electron was ~5 ms and over this time scale we did not observe any additional heme oxidation.

Summary

An activated form of the oxidized Cyt*c*O, $\mathbf{O_H}$, was postulated. The difference between states **O** and $\mathbf{O_H}$ was suggested to be an elevated midpoint potential of Cu_B in the latter. In the present study, we used an alternative experimental technique to approach the problem and found that in the $\mathbf{O_H}$ state the electron resides mainly at heme *a* and Cu_A. In other words the Cu_B midpoint potential was not elevated in $\mathbf{O_H}$. A similar behavior was observed in native membrane, which excludes the possibility that the behavior is due to removal of lipids from the protein.

Materials and Methods

Preparation of *R. sphaeroides* CytcO. The *R. sphaeroides* bacteria were grown aerobically in the dark at 30 °C in a Sistrom medium. After harvesting, the cells were re-suspended in 50 mM Tris-buffer, pH 8.0 (0.2 g/ml) and stirred for one hour at 4 °C in the presence of DNase I (0.05 mg/ml final concentration). The suspension was subsequently passed twice through a continuous-flow cell disruptor (Constant Systems LTD) operating at 170 MPa. Unbroken bacteria and cell debris were removed from the suspension by low-speed ultra-centrifuging (7800 g for 15 min at 4 °C) followed by high-speed ultra-centrifugation (138 000 g for 90 minutes at 4 °C) to collect the membrane fraction. The membrane pellet was re-suspended (homogenized) in 50 mM Tris-buffer.

For purification of the Cyt*c*O the membrane fraction of the cells was solubilized in 1.5% *n*-dodecyl β -D-maltoside (DDM). The histidine-tagged Cyt*c*O was purified using Ni^{2+}-NTA affinity chromatography as described previously[43,44].

Measurement of the oxidation kinetics. For studies of Cyt*c*O in the native membrane environment the *R. sphaeroides* membranes were diluted to ~5 μM Cyt*c*O in 20 mM HEPES (pH 7.5) and 100 μM EDTA.

For studies of the purified Cyt*c*O, the buffer-solution of the enzyme was exchanged for 20 mM HEPES (pH 7.5), 0.05% DDM and 100 μM EDTA using a gel filtration column (PD-10, GE Healthcare), resulting in a final Cyt*c*O concentration of ~10 μM. The same method was used to prepare the cyt. *c*-Cyt*c*O complex where equine heart cyt. *c* (Sigma-Aldrich) was added to the Cyt*c*O prior application to the PD-10 column. For the *R. sphaeroides* membrane fraction, the equine heart cyt. *c* was added directly to the sample.

The cyt. *c*-Cyt*c*O ratio was 1.2–1.3 (see text and figure legends). The sample was transferred to a locally modified Thunberg cuvette after which air in the cuvette was exchanged for N_2 using a vacuum line. The sample was reduced upon anaerobic addition of ascorbate (2 mM) and the redox mediator hexa-ammine-ruthenium(II) chloride (1 μM). After full reduction, the N_2 atmosphere in the cuvette was replaced by carbon monoxide, which binds to the reduced heme a_3. The redox state of the enzyme as well as formation of the Cyt*c*O-CO complex were verified spectrophotometrically.

The Cyt*c*O-CO complex (with or without cyt. *c*) was mixed rapidly with an oxygen-saturated buffer (20 mM HEPES (pH 7.5), 0.05% DDM, 0.1 mM EDTA) at a Cyt*c*O:O_2-saturated solution ratio of 1:5) in a flow-flash apparatus (Applied Photophysics). The CO ligand was photo-dissociated from heme a_3, about 200 ms after mixing, by means of a 10-ns laser flash (Quantel Brilliant B, Nd-YAG, 532 nm), enabling oxygen to bind to heme a_3. The subsequent reaction of the reduced Cyt*c*O with oxygen was monitored as absorbance changes over time at different single wavelengths[45].

References

1. Kaila, V. R. I., Verkhovsky, M. I. & Wikström, M. Proton-coupled electron transfer in cytochrome oxidase. *Chem. Rev.* **110**, 7062–7081 (2010).
2. Hosler, J. P., Ferguson-Miller, S. & Mills, D. A. Energy transduction: Proton transfer through the respiratory complexes. *Annual Review of Biochemistry* **75**, 165–187 (2006).
3. Yoshikawa, S. *et al.* Proton pumping mechanism of bovine heart cytochrome c oxidase. *Biochimica et Biophysica Acta - Bioenergetics* **1757**, 1110–1116 (2006).
4. Namslauer, A. & Brzezinski, P. Structural elements involved in electron-coupled proton transfer in cytochrome c oxidase. *FEBS Lett* **567**, 103–110 (2004).
5. Brzezinski, P. & Gennis, R. B. Cytochrome c oxidase: exciting progress and remaining mysteries. *J. Bioenerg. Biomembr.* **40**, 521–531 (2008).
6. Brzezinski, P. & Ädelroth, P. Design principles of proton-pumping haem-copper oxidases. *Curr Opin Struct Biol* **16**, 465–472 (2006).
7. Richter, O. M. H. & Ludwig, B. Electron transfer and energy transduction in the terminal part of the respiratory chain - Lessons from bacterial model systems. *Biochimica et Biophysica Acta - Bioenergetics* **1787**, 626–634 (2009).
8. Ferguson-Miller, S., Hiser, C. & Liu, J. Gating and regulation of the cytochrome c oxidase proton pump. *Biochimica et Biophysica Acta - Bioenergetics* **1817**, 489–494 (2012).

9. Rich, P. R. & Maréchal, A. Functions of the hydrophilic channels in protonmotive cytochrome c oxidase. *Journal of the Royal Society Interface* **10**, 183–196 (2013).
10. Konstantinov, A. A. Cytochrome c oxidase: Intermediates of the catalytic cycle and their energy-coupled interconversion. *FEBS Lett.* **586**, 630–639 (2012).
11. Blomberg, M. R. A. & Siegbahn, P. E. M. Proton pumping in Cytochrome c oxidase: Energetic requirements and the role of two proton channels. *Biochimica et Biophysica Acta (BBA) - Bioenergetics* **1837**, 1165–1177, https://doi.org/10.1016/j.bbabio.2014.01.002 (2014).
12. Popović, D. M., Leontyev, I. V., Beech, D. G. & Stuchebrukhov, A. A. Similarity of cytochrome c oxidases in different organisms. *Proteins: Structure, Function and Bioinformatics* **78**, 2691–2698 (2010).
13. Von Ballmoos, C., Ädelroth, P., Gennis, R. B. & Brzezinski, P. Proton transfer in ba_3 cytochrome *c* oxidase from *Thermus thermophilus*. *Biochim. Biophys. Acta* **1817**, 650–657 (2012).
14. Wikström, M., Sharma, V., Kaila, V. R. I., Hosler, J. P. & Hummer, G. New perspectives on proton pumping in cellular respiration. *Chem. Rev.* **115**, 2196–2221, https://doi.org/10.1021/cr500448t (2015).
15. Wikström, M. & Morgan, J. E. The dioxygen cycle. Spectral, kinetic, and thermodynamic characteristics of ferryl and peroxy intermediates observed by reversal of the cytochrome oxidase reaction. *J Biol Chem* **267**, 10266–10273 (1992).
16. Wikström, M. Identification of the electron transfers in cytochrome oxidase that are coupled to proton-pumping. *Nature* **338**, 776–778 (1989).
17. Wikström, M. *et al*. Mechanism of Proton Translocation by the Respiratory Oxidases - the Histidine Cycle. *Biochim. Biophys. Acta-Bioenerg.* **1187**, 106–111 (1994).
18. Verkhovsky, M. I., Jasaitis, A., Verkhovskaya, M. L., Morgan, J. E. & Wikström, M. Proton translocation by cytochrome c oxidase. *Nature* **400**, 480–483 (1999).
19. Bloch, D. *et al*. The catalytic cycle of cytochrome c oxidase is not the sum of its two halves. *Proc. Natl. Acad. Sci. USA* **101**, 529–533 (2004).
20. Wikström, M. & Verkhovsky, M. I. Towards the mechanism of proton pumping by the haem-copper oxidases. *Biochimica et Biophysica Acta - Bioenergetics* **1757**, 1047–1051 (2006).
21. Belevich, I., Bloch, D. A., Belevich, N., Wikström, M. & Verkhovsky, M. I. Exploring the proton pump mechanism of cytochrome c oxidase in real time. *Proc. Natl. Acad. Sci. USA* **104**, 2685–2690 (2007).
22. Sharma, V., Karlin, K. D. & Wikström, M. Computational study of the activated OH state in the catalytic mechanism of cytochrome c oxidase. *Proc. Natl. Acad. Sci. USA* **110**, 16844–16849, https://doi.org/10.1073/pnas.1220379110 (2013).
23. Blomberg, M. R. A. & Siegbahn, P. E. M. Protonation of the binuclear active site in cytochrome c oxidase decreases the reduction potential of Cu B. *Biochimica et Biophysica Acta - Bioenergetics* **1847**, 1173–1180, https://doi.org/10.1016/j.bbabio.2015.06.008 (2015).
24. Jancura, D. *et al*. Spectral and kinetic equivalence of oxidized cytochrome c oxidase as isolated and "activated" by reoxidation. *J. Biol. Chem.* **281**, 30319–30325, https://doi.org/10.1074/jbc.M605955200 (2006).
25. Brand, S. E. *et al*. A new ruthenium complex to study single-electron reduction of the pulsed OH state of detergent-solubilized cytochrome oxidase. *Biochemistry* **46**, 14610–14618, https://doi.org/10.1021/bi701424d (2007).
26. Hill, B. C. Modeling the sequence of electron transfer reactions in the single turnover of reduced, mammalian cytochrome c oxidase with oxygen. *J Biol Chem* **269**, 2419–2425 (1994).
27. Hill, B. C. The reaction of the electrostatic cytochrome c-cytochrome oxidase complex with oxygen. *J. Biol. Chem.* **266**, 2219–2226 (1991).
28. Hirota, S. *et al*. A flash-photolysis study of the reactions of a caa3-type cytochrome oxidase with dioxygen and carbon monoxide. *J Bioenerg Biomembr* **28**, 495–501 (1996).
29. Brzezinski, P. & Larsson, G. Redox-driven proton pumping by heme-copper oxidases. *Biochim. Biophys. Acta* **1605**, 1–13 (2003).
30. Einarsdóttir, Ó. Fast Reactions of Cytochrome-Oxidase. *Biochim. Biophys. Acta* **1229**, 129–147 (1995).
31. Karpefors, M., Ädelroth, P., Zhen, Y., Ferguson-Miller, S. & Brzezinski, P. Proton uptake controls electron transfer in cytochrome c oxidase. *Proc. Natl. Acad. Sci. USA* **95**, 13606–13611 (1998).
32. Liao, G. L. & Palmer, G. The reduced minus oxidized difference spectra of cytochromes a and a3. *Biochim. Biophys. Acta* **1274**, 109–111 (1996).
33. Vanneste, W. H. The stoichiometry and absorption spectra of components a and a-3 in cytochrome c oxidase. *Biochemistry* **5**, 838–848 (1966).
34. Szundi, I., Liao, G. L. & Einarsdóttir, O. Near-infrared time-resolved optical absorption studies of the reaction of fully reduced cytochrome c oxidase with dioxygen. *Biochemistry* **40**, 2332–2339, https://doi.org/10.1021/bi002220v (2001).
35. Gorbikova, E. A., Vuorilehto, K., Wikström, M. & Verkhovsky, M. I. Redox titration of all electron carriers of cytochrome c oxidase by Fourier transform infrared spectroscopy. *Biochemistry* **45**, 5641–5649, https://doi.org/10.1021/bi060257v (2006).
36. Sousa, F. L. *et al*. Redox properties of thermus thermophilusba3: Different electron-proton coupling in oxygen reductases? *Biophys. J.* **94**, 2434–2441 (2008).
37. Melin, F. *et al*. The unusual redox properties of C-type oxidases. *Biochimica et Biophysica Acta - Bioenergetics* **1857**, 1892–1899, https://doi.org/10.1016/j.bbabio.2016.09.009 (2016).
38. Alric, J. *et al*. Electrostatic interaction between redox cofactors in photosynthetic reaction centers. *J. Biol. Chem.* **279**, 47849–47855, https://doi.org/10.1074/jbc.M408888200 (2004).
39. Öjemyr, L. N., Von Ballmoos, C., Faxén, K., Svahn, E. & Brzezinski, P. The membrane modulates internal proton transfer in cytochrome c oxidase. *Biochemistry* **51**, 1092–1100 (2012).
40. Näsvik Öjemyr, L., Lee, H. J., Gennis, R. B. & Brzezinski, P. Functional interactions between membrane-bound transporters and membranes. *Proc Natl Acad Sci USA* **107**, 15763–15767 (2010).
41. Wittenberg, B. A. & Wittenberg, J. B. Transport of oxygen in muscle. *Annual Review of Physiology* **51**, 857–878 (1989).
42. Wikström, M. Active site intermediates in the reduction of O 2 by cytochrome oxidase, and their derivatives. *Biochimica et Biophysica Acta - Bioenergetics* **1817**, 468–475 (2012).
43. Mitchell, D. M. & Gennis, R. B. Rapid purification of wildtype and mutant cytochrome c oxidase from Rhodobacter sphaeroides by Ni(2+)-NTA affinity chromatography. *FEBS Lett.* **368**, 148–150 (1995).
44. Zhen, Y. *et al*. Overexpression and purification of cytochrome coxidase from Rhodobacter sphaeroides. Protein Expression and Purification. *Protein Expr. Purif.* **13**, 326–336 (1998).
45. Brändén, M. *et al*. On the role of the K-proton transfer pathway in cytochrome c oxidase. *Proc. Natl. Acad. Sci. USA* **98**, 5013–5018 (2001).
46. Van Gelder, B. F. & Slater, E. C. The extinction coefficient of cytochrome c. *BBA - Biochimica et Biophysica Acta* **58**, 593–595 (1962).
47. Boelens, R. & Wever, R. Redox reactions in mixed-valence cytochrome c oxidase. *FEBS Lett.* **116**, 223–226, https://doi.org/10.1016/0014-5793(80)80649-1 (1980).

Acknowledgements

We would like to thank Margareta Blomberg and Pia Ädelroth for valuable discussions. The study was supported by grants from the Swedish Research Council and the Knut and Alice Wallenberg Foundation.

Author Contributions

J.V. performed experiments. P.B. and J.V. wrote the manuscript and prepared figures. R.B.G., P.B. and J.V. planned research. All authors reviewed the manuscript.

Additional Information

Competing Interests: The authors declare no competing interests.

Publisher's note: Springer Nature remains neutral with regard to jurisdictional claims in published maps and institutional affiliations.